ELSEVIER

Geoderma 108 (2002) 207–223

GEODERMA

www.elsevier.com/locate/geoderma

Macropore transport of bromide as influenced by soil structure differences

Sabit Ersahin [a,*], Robert I. Papendick [b], Jeffrey L. Smith [b], C. Kent Keller [c], Valipuram S. Manoranjan [d]

[a] *Department of Soil Science, Faculty of Agriculture, Gaziosmanpasa University, Tokat 60200, Turkey*
[b] *USDA/ARS, Washington State University, Pullman, WA 99164-6421, USA*
[c] *Department of Geology, Washington State University, Pullman, WA 99164-2812, USA*
[d] *Department of Pure and Applied Mathematics, Washington State University, Pullman, WA 99164-3113, USA*

Received 30 March 2001; received in revised form 28 September 2001; accepted 8 February 2002

Abstract

Macropore transport of chemicals in soil often causes unexpected contamination of groundwater. The effect of soil structure on the functions of various sized macropores was assessed, investigating transport of nonreactive bromide (Br) under matric heads of 0, −2, −5 and −10 cm using undisturbed soil columns from A, B_w and E horizons of a Thatuna silt loam soil (fine-silty, mixed, mesic Xeric Argialbolls). The experimental breakthrough curves (BTC) for Br were described with a two-region physical nonequilibrium model. Greatest macroporosity occurred in the A horizon and lowest in the E horizon. The measured pore water velocity v under saturated conditions ranged from 18.92 cm day^{-1} in the E horizon to 64.28 cm day^{-1} in the A horizon. While the greatest dispersivity λ occurred in the B_w horizon due to medium subangular blocky and prizmatic aggregates, the lowest dispersivity occurred in the E horizon due to its low macroporosity and massive structure. The fitted mobile water partitioning coefficient β ranged from 0.30 in the A horizon under 0 cm matric head to 0.93 in the E horizon under 0 cm matric head. The calculated values of rate of diffusive mass exchange α decreased with decreasing matric head in A and B_w horizons, and slightly increased and then decreased in the E horizon. The difference among each of the values of the parameters v, β, α and λ for the A, B_w and E horizons was greatest under saturated conditions. However, gradually decreasing matric head until about −3 cm decreased the difference among the values for a particular parameter for different horizons, sharply. The difference remained fairly unchanged with further decreases in the matric head, suggesting that most of the variability in macropore transport of bromide for these horizons caused by pores with radii larger than about 0.5 mm. In A and B_w horizons, there was a sudden change in soil solution movement between −2 and −5 cm matric head, indicating that macropore flow generally occurred at matric heads greater than

* Corresponding author. Fax: +356-252-1488.
E-mail address: sersahin@gop.edu.tr (S. Ersahin).

PII: S0016-7061(02)00131-3

– 5 cm in the A and B_w horizons. However, decreasing matric head had no effect on mobile water content of the columns from the E horizon. It was concluded that macropore transport of nonreactive solutes generated in the A and B_w horizons may be hampered in the E horizon. Therefore, the depth, thickness and position of the E horizon should be considered in studies targeted to modeling macropore transport of nonreactive chemicals in the soils of Thatuna Series.

Keywords: Macropore; Soil structure; Bromide transport; Two-region model; Breakthrough curve

1. Introduction

Macropores have a considerable effect on water transmission in soils with high water potentials. Although macropores represent a small portion of a soil porosity, they contribute an important fraction of solute transported near saturation (Luxmoore, 1981). To understand their influence on chemical transport, the water flow effects of macropores near saturation should be recognized well (Angulo-jaramillo et al., 1996).

The term macropore refers to relatively large noncapillary pores or channels formed by both biological and nonbiological activities. Macropores may range from 0.03 to a few centimeters in diameter or cross-section, and the number of macropores within each radius class can be highly variable over a small area (Luxmoore, 1981; Beven and Germann, 1982).

Macropores can be characterized by physical and morphometric techniques (Bouma, 1977, 1991). However, results showed that the macroporosity obtained by soil physical technique was generally greater than that obtained by morphometric methods (Bouma, 1977). This should be considered in correlating soil macroporosity with transport processes in soil physics studies.

A description of soil macropore features and their influence on water and chemical movement through the soil profile can be obtained through miscible displacement experiments (Nielsen and Biggar, 1962). Miscible displacement experiments not only provide information on the soil macropore function, but also on other processes such as hydrodynamic dispersion, diffusion, ion exchange and adsorption phenomena for solute transport under various flow rate and water content conditions. For example, in general, when the dispersion coefficient is small with respect to the advective velocity, the experimental breakthrough curves (BTC) for an instantaneous release of a nonreactive solute at a point in an uniform flow field will be symmetrical, reflecting the conditions for "equilibrium/ideal" solute transport. However, when the dispersion coefficient is high (e.g. macropore flow and intraaggregate diffusion), BTCs obtained will be asymmetric, showing early breakthrough and tailing that are caused by conditions favoring "non-equilibrium/nonideal" solute transport (Sugita and Gillham, 1995). In general, the macropore effect causes early appearance, and intraaggregate diffusion causes tailing of the tracer chemical.

Miscible displacement experiments have been used by many researchers to quantitatively and qualitatively describe soil structure effect on solute transport. In their early work, Biggar and Nielsen (1962) determined the effect of hydrodynamic dispersion and diffusion of the tracer chemical on the solute transport. They concluded that the shape of

the BTCs depends on microscopic flow velocity distribution, and that one of the most important soil physical properties was the amount of water that was not readily displaced. Nielsen and Biggar (1962) showed that increasing aggregate size favored early appearance of the tracer in the effluent from miscible displacement experiments, indicating the effect of preferential flow. Anderson and Bouma (1977a,b) observed hydrodynamic dispersion in different undisturbed soils having identical texture, but with different structures under saturated and unsaturated flow conditions. They concluded that differences in dispersion were clearly related to differences in soil structure and that routine soil structure descriptions would be potentially useful as a correlative tool to predict certain aspects of physical behaviors of the soils. Anomosa et al. (1990) evaluated the effect of macropores and regions of immobile water through miscible displacement tests. They showed that approximately 50% of total water was in immobile water regions in the soil. They emphasized that the soil structural properties have a considerable effect on rapid transport of solutes. Jardine et al. (1993) conducted miscible displacement experiments where reactive and nonreactive tracers were displaced in large undisturbed soil columns subjected to various soil water matric heads. They found that most of the water flow was channeling through pores larger than 0.30 mm in diameter. Li and Ghodrati (1994) applied miscible displacement technique to study functions of macropores formed by alfalfa, corn and wheat roots. They emphasized that like wheat roots, both alfalfa and corn roots can form well-connected macropores that can initiate macropore flow under soil matric heads greater than -10 cm, giving an effective pore diameter of 0.3 mm.

Studies on macropore flow have generally been conducted at soil matric heads greater than -10 cm. Seyfried and Rao (1987) found significant preferential flow at water potentials of 0 and -1 cm, indicating macropore effect. They observed that when matric head of soil water lowered to -10 cm, the preferential flow effect vanished, suggesting that pores having diameters smaller than 0.3 mm did not contribute to preferential flow. Langner et al. (1999) found that fitting results of observed breakthrough curves (BTC) at $h \leq -10$ cm indicated absence of preferential flow. However, experiments at $h \geq -5$ cm consistently exhibited physical nonequilibrium conditions, indicating the presence of macropore effect. Angulo-jaramillo et al. (1996) observed that the soil water flow changed to a macroporosity flow when the matric head increased from -10 to 0 cm, resulting in an abrupt decrease in mobile water ratio from 0.37 to 0.11. They suggested that for a given porous network topology, the mobile water content would depend both on the dynamic of the water movement and on the connectivity of the porous network.

The objective of this study was to assess the effect of soil structure on macropore transport of bromide in A, B_w and E horizons of sloping Thatuna silt loam soil, one of the largest and well-developed soil series of Palouse Region of Washington State.

2. Materials and methods

2.1. Site description

The study site was on a north-facing slope (back slope) on the Palouse USDA-ARS Conservation Research Station, located ~ 3 km north of Pullman, Washington (SW 1/4,

sec. 19, T15N, R45E). The soil is a Thatuna series (fine-silty, mixed, mesic Xeric Argiallbolls) which includes gently sloping to very steep (7–25%), well-drained soils formed from loess on north and east slopes of the Palouse landscape (Donaldson, 1980; Busacca and Montgomery, 1992).

The Thatuna series has three major horizons. These include a well-structured A horizon and a cambic B (B_w) horizon overlying a distinct albic (E) horizon (Busacca and Montgomery, 1992).

The climate is Mediterranean type with cold-wet winters and dry-warm summers. The annual precipitation is about 550 mm, most of which occurs in the late fall, winter and early spring. Within the study area, variations in microclimate result in differences in native vegetation and soil profile characteristics over short distances (Donaldson, 1980; Busacca and Montgomery, 1992).

The study site was a grassland. The A horizon is characterized by a dark grayish brown color (10YR4/2; dry); moderate fine and medium granular structure; common fine and very fine roots; common fine pores. The B_w horizon is characterized by a dark brown color (10YR4/3; dry); moderate medium and weak medium prismatic and subangular blocky structure; many fine and very fine pores. The E horizon is characterized by a light gray color (10YR7/1; dry); massive, soft, loose structure; very friable, slightly sticky and slightly plastic; common fine iron manganese concretions (Ersahin, 1996).

2.2. Physical and chemical properties of the soils

Selected physical and chemical properties of the soil horizons are presented in Table 1. Bulk density increases with depth. The E horizon has the highest bulk density. The silt fraction is dominant throughout soil profile. Sand contents remain the same with depth until the lower end of the B_w horizon, then decrease in the E horizon. Clay content remains constant until the lower end of the B_w horizon and then slightly increases in the E horizon. Values for pH gradually increase, and for CEC gradually decrease with depth, attributable to the gradual decrease in the values for organic carbon.

2.3. Sampling

The soil profile was excavated to a depth below the E horizon to determine the depth of each soil horizon. Four replicated undisturbed soil cores, 72 mm diameter and 90 mm length, were obtained with a tractor-mounted coring machine from the A, B_w and E

Table 1
Selected physical and chemical properties of the soils

Horizon	Depth (cm)	Sampling depth (cm)	Particle size distribution (%)			BD (mg m^{-3})	CEC (Mol_c kg^{-1})	EC (S m^{-1})	OC (%)	pH
			Sand	Silt	Clay					
A	0–30	8–17	30.8	62.0	7.2	1.18	0.22	0.02	1.88	6.35
B_w	31–90	40–49	31.8	61.0	7.2	1.20	0.14	0.01	1.85	6.88
E	91–110	97–106	25.4	66.4	8.2	1.41	0.10	0.02	0.30	7.10

BD: bulk density, CEC: cation exchange capacity, EC: electrical conductivity, OC: organic carbon.

horizons. The soil cores were trimmed at the end of the steel sampler after which their ends were closed with plastic cups and stored at 2 °C in a temperature controlled room.

2.4. Miscible displacement experiments and soil macroporosity

Before conducting a miscible displacement experiment, both ends of the soil column were capped with filter discs formed from quick setting porous cement (Booltink et al., 1991), and each disc having an outlet. The core was then gradually saturated with 0.01 M $CaCl_2$ solution from the bottom of the column (van Genuchten and Wierenga, 1977). Upon saturation, the core was sealed around the edge with silicon rubber and positioned on an upright stand. The inlet at the top of the column was connected to a tension infiltrometer, and the outlet at the bottom was connected to a vacuum chamber which enclosed an automatic fraction collector. Saturated hydraulic conductivity of each column was determined with the tension infiltrometer using zero tension. After the flow rate was established, the top outlet of the column was connected to a syringe pump. Approximately 1.5 pore volumes of tracer solution of 0.05 M KBr in 0.01 M $CaCl_2$ solution were introduced into the column with the syringe pump followed by approximately 3 pore volumes of 0.01 M $CaCl_2$ to leach the tracer from the column. The effluent was collected using the automatic fraction collector, and analyzed for bromide using an ion-specific electrode (Abdalla and Lear, 1975).

After the experiment was completed for the saturated conditions, the column was leached extensively with leaching solution to minimize the background effect of bromide on the next experiment. The column was extracted by applying -2 cm matric head to the both ends of the vertical column, and the experiment was repeated. Similarly, the experiment was repeated with the same column under -5 and -10 cm matric heads. Water extracted at each of -2, -5 and -10 cm matric heads was collected and measured to calculate the volume of macropores drained at each step. The soil core was detached from the system, and its water content was determined. The water content determined after -10 cm matric head experiment was the amount of one pore volume of the column under -10 cm matric head. The pore volume of the column under -5 cm matric head was calculated by adding the amount of the water released between -5 and -10 cm to the pore volume calculated for -10 cm matric head, and similarly for the -2 and 0 cm matric heads. Each time, results of the miscible displacement tests for four replicated cores were averaged and than fitted to obtain horizon-averaged parameters.

The volume of macropores controlling flow between -10 and -5 cm matric heads was calculated from the amount of water extracted between -5 and -10 cm matric heads, and similarly, the volume of macropores controlling flow between -10 and -2 cm matric heads was calculated from the amount of water extracted between -10 and -2 cm matric heads, and so on. Total macroporosity was calculated from total amount of water extracted (beginning with saturation) under -10 cm soil water matric head. For this experiment, we chose the macropore limit to be pores that emptied at -10 cm matric head (Ranken, 1974; Beven and Germann, 1982).

The relative concentrations (C/C_o) of Br were determined by dividing the concentration of the tracer of the effluent collected by the concentration of the tracer in the stock solution.

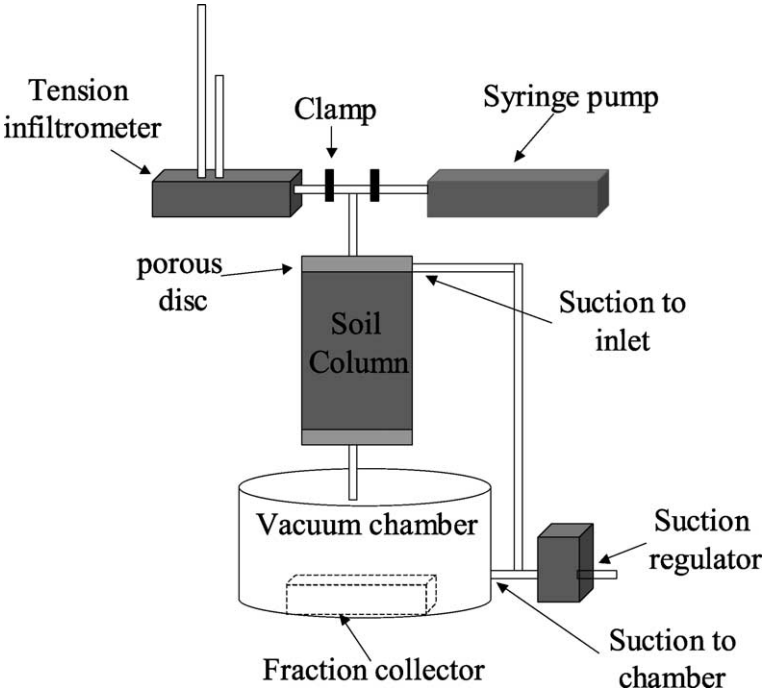

Fig. 1. The schematic of apparatus used to conduct miscible displacement experiments.

The apparatus used in this experiment was a combination of those described by Wierenga et al. (1973), Booltink et al. (1991) and Jardine et al. (1993) (Fig. 1). The tension infiltrometer was used to determine the flow rate of the column under the desired matric head. In order to maintain a unit potential gradient along the column, the same magnitude of matric head was applied to the both ends of the vertical column. During the experimentation, both inlet matric head and the outlet matric head was maintained by a vacuum source controlled by a suction regulator. The use of the syringe pump made it possible to maintain a constant inflow during the duration of experimentation (lasting up to two months).

The data from the flow experiments were quantitatively evaluated using the computer program CXTFIT (Parker and van Genuchten, 1984). The two-region (physical non-equilibrium) model was fitted to the data from experimental BTCs. The model parameters were obtained as follows. The fraction of mobile water content β (dimensionless), the coefficient of lateral mass exchange ω (dimensionless), and the coefficient of hydrodynamic dispersion D ($cm^2\ day^{-1}$) were fitted; the pore water velocity v ($cm\ day^{-1}$) and pulse duration T_0 (dimensionless) were measured. Retardation coefficient R (dimensionless) was assumed unity for nonreactive bromide. The rate coefficient of lateral transport α (day^{-1}) was calculated using the following equation,

$$\alpha = (q\omega)/L, \tag{1}$$

where L is the length of column (cm) and q is the specific discharge (cm day^{-1}) (van Genuchten, 1981; Parker and van Genuchten, 1984; Toride et al., 1995).

Dispersivity λ (cm) was calculated using the following relationship

$$\lambda = D/v. \quad (2)$$

2.5. Other soil analyses

Other soil analyses included soil bulk density by the core method (Blake and Hartge, 1986), particle size distribution by the hydrometer method (Gee and Bauder, 1986), water retention at -10, -33 and -100 kPa with standard pressure plate apparatus (Klute, 1986), organic matter contents by the Walkley–Black method (Jackson, 1956), pH with the standard glass electrode (McLean, 1982), EC with glass electrode (Rhoades, 1982) and cation exchange capacity by the method from Gillman (1979).

3. Results and discussion

3.1. Soil macroporosity

Macroporosity, defined as the average pore space (%) occupied by pores having radii larger than 0.15 mm, decreased with depth (Table 2) for all the matric heads. The highest macroporosity was in the A horizon, and the lowest was in the E horizon. The low macroporosity of the E horizon may be attributed to its high bulk density and massive structure.

Macropore size-distribution varied by horizon. In the A horizon, of the macropores, 16% (Table 2) were larger than 0.75 mm (in radius), 47% were between 0.3 and 0.75 mm and rest were between 0.15 and 0.3 mm; compared to those in the E horizon where 7% of the macropores had radii larger than 0.75 mm, 39% had radii between 0.3 and 0.75 mm and rest of the macropores had radii between 0.15 and 0.3 mm; indicating that compared with the A, the E horizon was dominated by relatively narrow macropores. The size-distribution of the macropores in the B_w horizon were between the A and E horizons.

3.2. Solute transport characteristics of the soil horizons

3.2.1. Soil macroporosity–pore water velocity relations

The pore water velocity v under saturated conditions decreased by horizon in the order of $A > B_w > E$ (Table 3). The greatest pore water velocity under saturated conditions

Table 2
Experimental conditions for the soil columns

Horizon	A	A	A	A	B_w	B_w	B_w	B_w	E	E	E	E
Matric head applied (cm)	0	−2	−5	−10	0	−2	−5	−10	0	−2	−5	−10
Macroporosity[a]	1.33	1.12	0.59	0.00	0.67	0.61	0.35	0.00	0.46	0.43	0.31	0.00

[a] Percent pore volume occupied by water filled macropores at the given soil matric head.

Table 3
Measured and two-region model-fitted parameters

Horizon	ψ (cm)[a]	v (cm d^{-1})[a]	D (cm^2 day^{-1})[b]	T_0[a]	β[b]	ω[b]	λ (cm)[c]	α (day^{-1})[c]	R^2
A	0	64.28 (21.97)[d]	42.66	1.54	0.30	2.47	0.68	11.28	0.999
A	2	27.31 (4.66)	35.80	1.56	0.81	0.85	1.22	1.67	0.985
A	5	13.15 (2.22)	18.38	1.69	0.87	0.59	1.39	0.54	0.989
A	10	4.71 (0.64)	3.32	1.51	0.86	1.24	0.70	0.41	0.998
B_w	0	23.53 (8.91)	24.30	1.42	0.53	0.70	1.03	1.64	0.997
B_w	2	12.97 (3.76)	20.78	1.73	0.75	0.98	1.60	0.90	0.979
B_w	5	8.90 (2.03)	10.02	1.96	0.78	0.91	1.12	0.61	0.976
B_w	10	5.39 (0.89)	5.61	1.57	0.78	1.51	1.05	0.57	0.987
E	0	18.92 (3.50)	10.37	1.37	0.93	0.51	0.55	0.35	0.995
E	2	12.30 (2.09)	6.65	1.37	0.90	1.00	0.54	0.44	0.976
E	5	6.83 (0.82)	2.90	1.36	0.91	0.98	0.42	0.42	0.988
E	10	4.75 (0.78)	2.17	1.40	0.92	1.27	0.45	0.39	0.984

ψ is the tension applied; v and D are the pore water velocity and hydrodynamic dispersion coefficients, respectively; T_0 is the dimensionless pulse duration; β is the dimensionless mobile water partitioning coefficient; ω is the dimensionless mass transfer coefficient between mobile and immobile regions; λ is the dispersivity; α is the rate coefficient for mass transfer between mobile and immobile regions; and R^2 is the coefficient of multiple determination.

[a] Measured.
[b] Fitted.
[c] Calculated from other parameters.
[d] Values in the parenthesis are standard deviations of four replications.

occurred in the A horizon. Application of -10 cm matric head decreased the pore water velocity more than 13-fold, although the volumetric water content decreased only by 1.3% (Table 2), suggesting that the water flux be predominantly controlled by the large pores. The experimental BTCs for the A horizon were the most asymmetric under saturated conditions (Fig. 2), indicating a greater effect of macropore flow on physical non-equilibrium in this horizon.

Application of -10 cm matric head decreased the pore water velocity approximately four times in the B_w horizon (Table 3). This suggest that only the largest pores in the B_w horizon are smaller than in the A horizon. Figs. 2 and 3 indicate an earlier breakthrough of tracer for the B_w horizon compared with the A under saturated conditions, although v for the A horizon under saturation was far greater than that for the B_w horizon. This greater nonuniformity in the experimental BTCs of the B_w horizon could be attributed to soil structural features. Morphological investigations revealed that the A horizon was dominated by small-to-medium spherical aggregates, whereas the B_w horizon was dominated by medium prismatic and subangular blocky aggregates. As matric head decreased, the early breakthrough decreased more rapidly in the A than in the B_w horizon. Rasmuson (1985) reported that for rapid flow experiments, the solute retention was nearly identical for spherical, platy, and cylindrical aggregates in fixed beds. However, for slow flow, the solute retention was greater for the platy than for cylindrical aggregates. Anderson and Bouma (1977a,b) observed considerable flow heterogeneity in the undisturbed soil columns dominated by medium subangular blocky structure under saturate and unsaturated conditions. Therefore, the earlier breakthrough under unsaturated conditions for the B_w

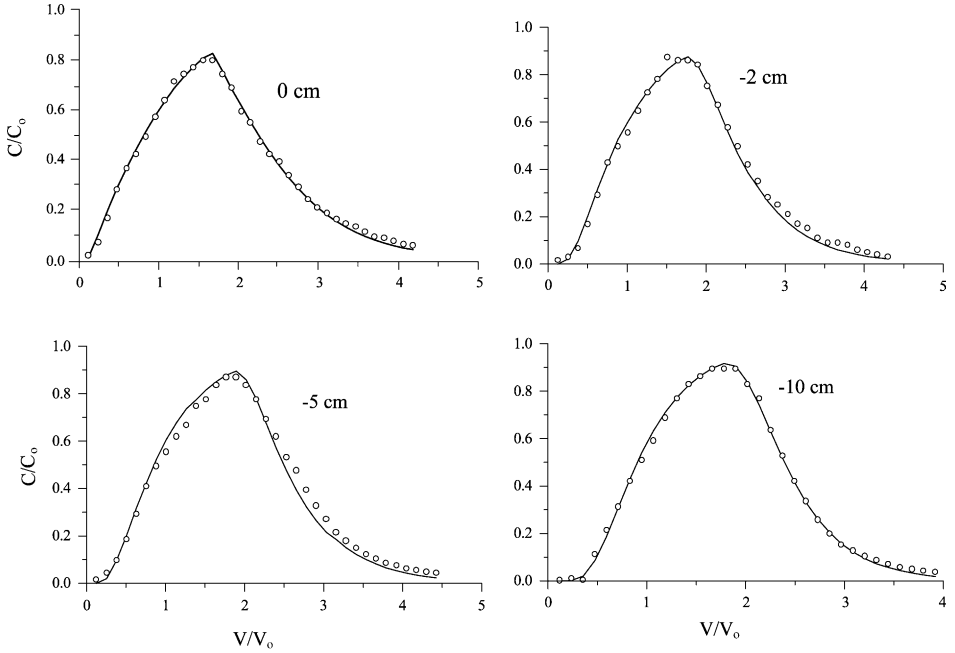

Fig. 2. Experimental and fitted breakthrough curves in the A horizon under 0, −2, −5 and −10 cm soil water matric heads. The circles represent experimental data points and lines were calculated with the two-region model.

horizon could be related to the presence of medium subangular blocky aggregates in this horizon. We notice from Fig. 3 that the experimental BTCs of bromide are not fairly symmetrical even under −10 cm matric head where macropore flow is supposed to vanish, indicating that there was still a nonuniformity in bromide transport possibly caused by the lateral mass exchange taking place between intraaggregate and interaggregate spaces.

The lowest *v* value at saturation occurred in the E horizon (Table 3). The BTCs for the E horizon under saturated conditions was quite symmetrical and showed no early appearance of the tracer (Fig. 4). Decreasing the matric head did not affect the shape of the BTCs, suggesting that the conditions for macropore transport be absent in the E horizon. The common fine iron manganese concretions observed by morphological investigation would be associated to the temporarily prevailing wet conditions due to relatively low permeability in the E horizon.

The relationship between *v* values and matric head (*h*) in A, B_w and E horizons varied (Fig. 5). We notice from Fig. 5 that difference in the *v* values of B_w and E horizons were not so high. However, *v* values for the A horizon were considerably higher than those for the B_w and E values under saturated conditions. As matric head decreased from 0 to around −3 cm, the gap in the *v* values decreased sharply. The A horizon had more macropores with radii lager than 0.75 mm (Table 2). Therefore, most of the difference in the macropore flow between the A horizon and B_w and E horizons was caused by macropores larger than about 0.5 mm in radius in the former.

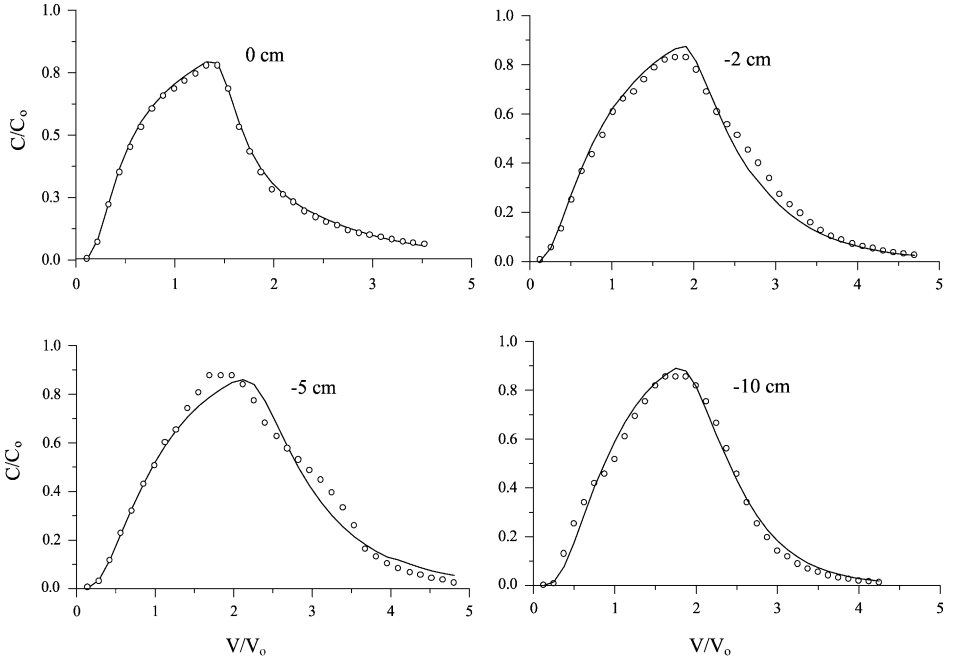

Fig. 3. Experimental and fitted breakthrough curves in the B_w horizon under 0, −2, −5 and −10 cm soil water matric heads. The circles represent experimental data points and lines were calculated with the two-region model.

3.2.2. Soil macroporosity–dispersivity relations

The values of dispersivity λ obtained at matric heads higher than −10 cm for the A and the B_w horizons were generally greater than unity (Table 3). This indicates that transport of bromide was dispersive dominated in these soils at high soil water potentials. The experimental BTCs at matric heads >-10 cm showed both early breakthrough and tailing (Figs. 2 and 3), which is indicative of both macropore flow and extensive mass exchange between mobile and immobile regions in these soils. In general, high values of pore water velocity matched with high values of hydrodynamic dispersion coefficient D for the A and B_w horizons (Table 3), suggesting that the transport of Br in these soils is more a function of physical characteristics of the porous medium than diffusive characteristics of Br. This relationship may have been masked by other effects such as film, axial, and intraparticulate diffusion in the E horizon, as noted by Brusseau (1993).

In contrast to the high D values for the A and B_w horizons, little dispersion occurred in the E horizons due to narrow pore size distributions (Tables 2 and 3). The low D values in the E horizons (Table 3) suggested that mass transport was more a function of convective flow than dispersive flow in this horizon. The experimental BTCs for this horizon showed little tailing and no early breakthrough (Fig. 4), indicating a more uniform solute front and lack of the conditions favoring macropore transport compared to those in the upper horizons.

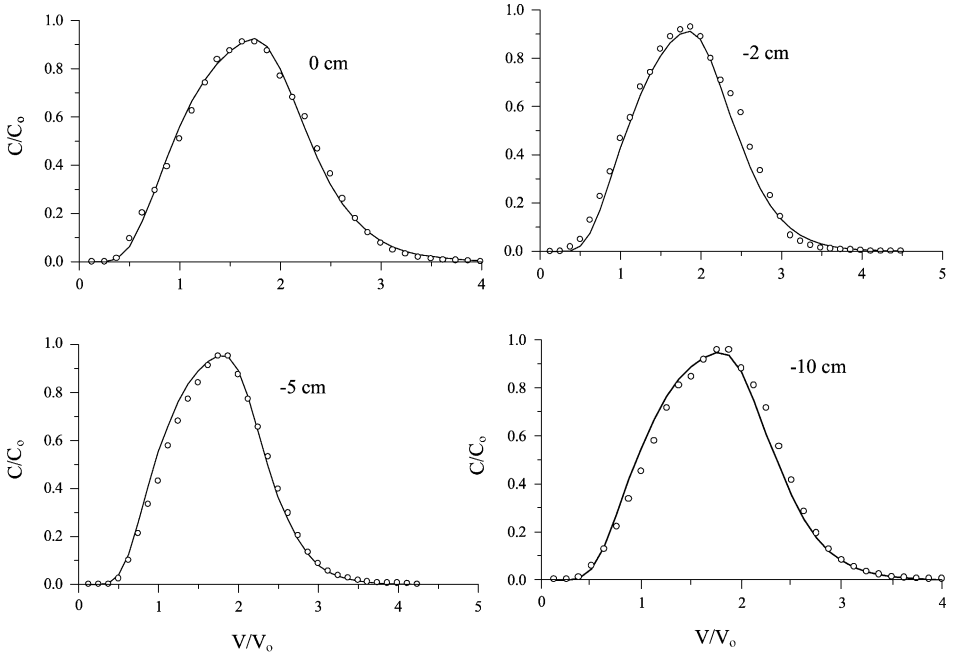

Fig. 4. Experimental and fitted breakthrough curves in the E horizon under 0, −2, −5 and −10 cm soil water matric heads. The circles represent experimental data points and lines were calculated with the two-region model.

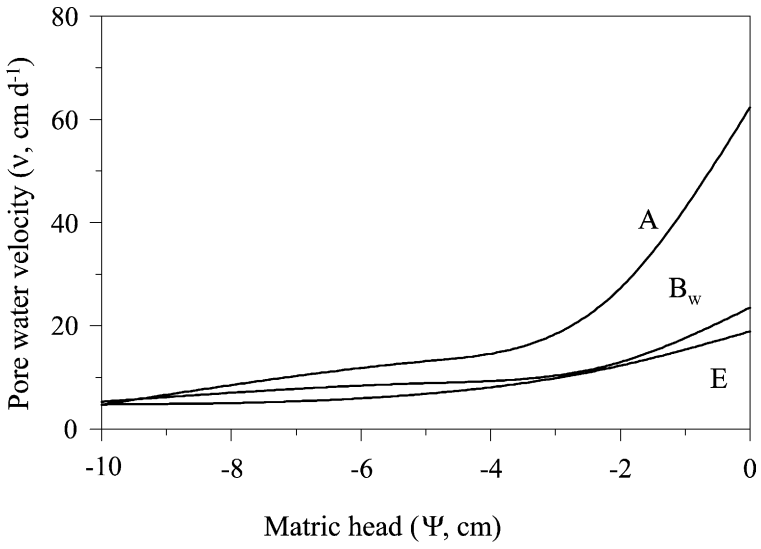

Fig. 5. Relationship between soil water matric head and pore water velocity.

3.2.3. Soil macroporosity–mobile water content relations

The model-fitted values of mobile water partitioning coefficient β under saturated conditions were 0.30 for the A, 0.53 for the B_w and 0.93 for the E horizon (Table 3). The large immobile water content obtained for the A horizon could be due to its high saturated pore water velocity caused by macropores. This relationship can be noticed when Figs. 5 and 6 are compared. Similar results have been reported elsewhere (Nikedi-Kizza et al. 1983). High immobile water contents despite the relatively low pore water velocities for the B_w horizon could be related to the presence of medium prismatic and subangular blocky aggregates in this horizon.

Decreasing the matric head had no effect on β values for the columns from the E horizon (Fig. 6). E horizon had narrower macropore size distribution compared with those of the A and the B_w horizons (Table 2); and had massive structure compared with small-to medium granular structure in the A horizon, and medium prismatic and subangular blocky structure in the B_w horizon. Therefore, high β values of the E horizon even under saturated condition could be related to its massive structure, and narrower pore size distribution.

The relationship between soil water matric head and β values in A, B_w and E horizons is presented in Fig. 6. Similar to pore water velocity values (Fig. 5), most of the variability in the β values for the horizons occurred matric heads greater than -3 cm. In A and B_w horizons, there was a sudden change in soil solution movement around the matric head of -3 cm. This gives an effective pore radius around 0.50 mm. The results of the present study indicate that mobile water regimes become more important at the matric heads above -3 cm. Similar results were reported elsewhere. For example, Langner et al. (1999) observed that immobile water regions developed at $h \leq -5$ cm did not participate in advective flow. Seyfried and Rao (1987) found that matric heads of 0 and -1 cm resulted in nonequilibrium conditions, however, matric head of -10 cm resulted in no nonequilibrium condition. In a disc infiltrometer study, Angulo-jaramillo et al. (1996)

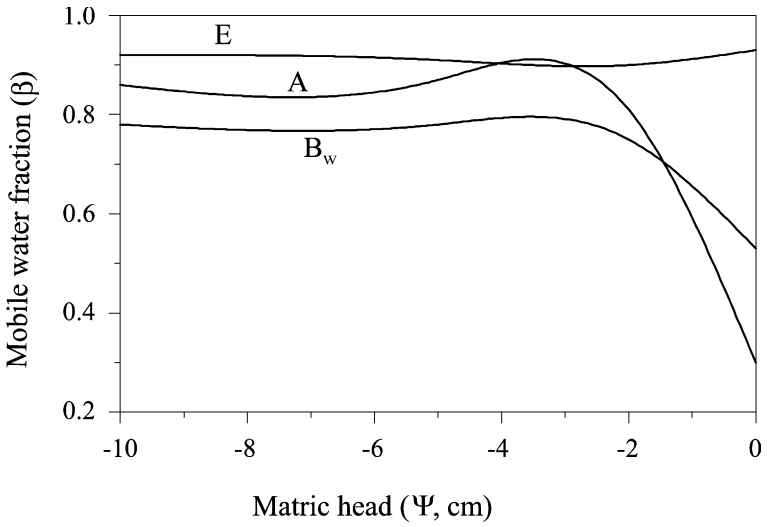

Fig. 6. Relationship between soil water matric head and mobile water partitioning coefficient.

observed that when matric head at tensiometer base changed from − 3 to − 6 cm, the flow was changed from gravity-dominated to capillary-dominated.

3.2.4. Soil macroporosity–lateral mass exchange relations

Generally, the estimated values for diffusive mass exchange ω increased slightly with decreasing matric head in each soil horizon, suggesting a greater mass exchange between mobile and immobile regions with longer residence time.

The parameter ω includes a rate coefficient α (day $^{-1}$), which controls rate of diffusive mass exchange between mobile and immobile regions (van Genuchten, 1981; Parker and van Genuchten, 1984; Toride et al., 1995). The pressure head effect on parameter α for each horizon is seen in Fig. 7. As soil matric head decreased to − 3 cm, the gap among the α values for the A horizon decreased sharply while values for other two horizons decreased only slightly. This was attributed to the effect of pore water velocity and mobile water content on α, greater pore water flux resulting greater α values and greater mobile water content resulting lower α values.

In general, the values of α decreased by horizon in the order A>B_w>E (Table 3). Large difference between the α values obtained for the A horizon under saturated and unsaturated conditions was again attributed, as suggested by Casey et al. (1998), to the large velocity difference between the mobile and immobile water regions. Similar results have been reported by others. For example, Casey et al. (1998) used a tension infiltrometer to measure soil hydraulic properties and transport parameters. Their results showed that a strong correlation occurred between soil water potential and values of α. They suggested that the correlation might be due to pressure head effect on soil water content which effects the flow velocity, which in turn has an effect on α. High values of α obtained for the A horizon under saturated conditions (Table 3) may also be attributed to its high immobile

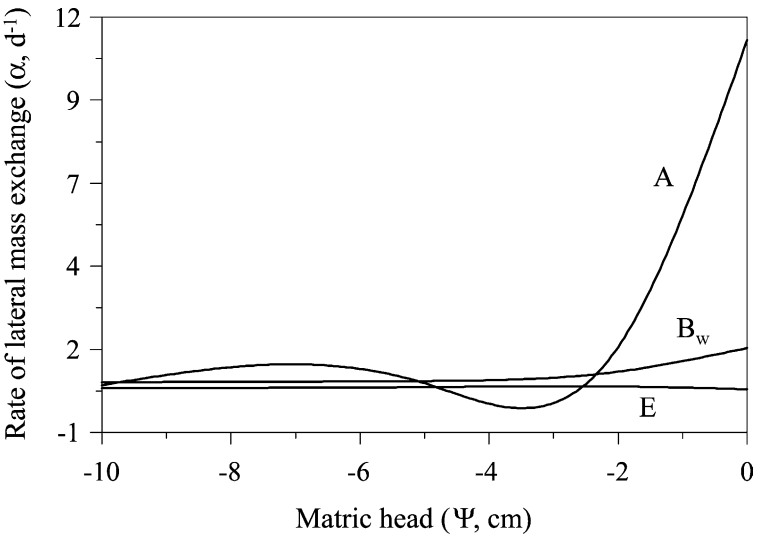

Fig. 7. Relationship between soil water matric head and coefficient of lateral mass exchange.

water content, and the platy and spherical aggregates which created a large surface area allowing intensive mass exchange between mobile (interaggregate) and immobile (intra-aggregate) regions.

The values of α for the B_w horizon under 0 and -2 cm water potential were considerably lower than those for the A horizon (Table 3 and Fig. 7). As suggested by Brusseau and Rao (1990), the relatively low values for α in the B_w horizon could be due to medium prismatic and subangular blocky aggregates with low surface-to-volume ratio which is characteristic of the soil structure in this horizon.

The values of α for the E horizon which were among the lowest in this study, again can be explained by its large mobile water content as stressed by Nikedi-Kizza et al. (1983) and Casey et al. (1998). This can be noticed when Figs. 6 and 7, where low values of α matched with high values of β, are compared. In addition, Rao et al. (1980) suggested that low flow velocity results in larger equilibrium times that cause smaller estimates of α. Therefore, the relatively low estimates of α obtained for the E horizon in the present study was attributed to its high mobile water content and to its relatively low flow velocity that resulted in larger equilibrium times.

Dye studies (Ersahin, 1996) conducted with the soil columns from B_w and E horizon showed that flow patterns were vertically oriented in these soils, indicating that as suggested by Anderson and Bouma (1977a) this allows to use relatively small cores in these soils. Also, standard deviation values calculated for pore water velocity values (Table 3) were not high, giving largest value for coefficient of variation (CV%) below 40%. Therefore, four replicated undisturbed columns (72 mm inner diameter and 90 mm length) used in this experiment should be representative for the soils studied.

Figs. 2–4 show a close association between fitted and experimental BTCs. In addition, the values for multiple determination coefficient R^2 are 0.99 in the majority of cases (Table 3), suggesting that the two-region model successfully described the results of miscible displacement tests in each case.

4. Summary and conclusions

Macropore transport of bromide (Br) as affected by soil structural differences was investigated using undisturbed soil cores for the A, B_w and E horizons (grassland over 20 years) of a Thatuna silt loam soil (fine-silty, mixed, mesic Xeric Argialbolls). Solute breakthrough curves (BTC) were obtained using undisturbed soil columns subjected to 0, -2, -5 and -10 cm soil water matric heads. Results from miscible displacement experiments were compared in terms of the relationships between soil macroporosity and nonuniformity in the transport of Br.

The most nonuniformity in Br transport occurred in the B_w horizon due to soil macropores and due to the presence of dominant medium prismatic and subangular blocky aggregates. The least occurred in the E horizon due to its narrow pore size distributions, and due to its massive structure.

Macroporosity was an important soil property affecting nonuniformity in Br transport. In general, high macroporosity resulted in high pore water velocities, dispersion of the

tracer, rate of lateral mass exchange between mobile and immobile regions, and immobile water content in the A and B_w horizons.

The difference among each of the values of the parameters pore water velocity v, fraction of mobile water content β, coefficient of lateral mass exchange α, and dispersivity λ for the A, B_w and E horizons was greatest under saturated conditions. However, the difference decreased sharply with decreasing matric head until about -3 cm, and remained fairly unchanged with further decreases in the matric head, suggesting that most of the variability in macropore transport of bromide for these horizons caused by pores with radii greater than about 0.5 mm.

Soil management may have a significant effect on structural features of soils, which in turn, considerably affects the macropore features such as type, shape, size, size distribution, origin, geometry and continuity of macropores. The soils (Thatuna silt loam) used in the present study were taken from a soil profile under a grassland for a long time (over 20 years). Since no grazing activities have been practiced on these soils, the whatever pore geometry existed remained intact for a long time. The Thatuna silt loam soils are also used for lentils, peas and alfalfa. Therefore, the same soils under adjacent tilled wheat field would yield quite different breakthrough characteristics especially for the upper A and B_w horizons due to the destroying effect of tillage on soil aggregates in the A horizon and compaction effect of plow tool under tillage depth. Also, Thatuna silt loam soils take place on gently sloping to steep (3–25% slopes) on the north-and east-facing side slopes. The thickness, depth, position, and structural features of the soil horizons may considerably vary based on the steepness and aspects of the slope due to the local differences in the rate of soil forming factors (i.e. differences in amount of water infiltrating into soil profile, evapotranspiration rate, topography, vegetation, etc.). Because of all these, we suggest that the results of the present study not be generalized over all the soils of the Thatuna silt loam series.

The results of this experiment are important, showing that the A, B_w and E horizons with different structure exhibited considerable differences in values for v, β and λ at matric head > -3 cm. The results further revealed that the macropore flow generated in the A and B_w horizon may be hampered in the underlying E horizon, suggesting that the position and depth of the E horizon be considered in the studies targeted to modeling macropore transport of nonreactive chemicals in the experimental soils.

Acknowledgements

We thank D.J. Mulla for his assistance for utilizing the CXTFIT model, and Debby Bikfasy and Jeff Boyle for their help in the laboratory analysis.

References

Abdalla, N.A., Lear, B., 1975. Determination of inorganic bromide in soils and plant tissues with a bromide selective-ion electrode. Commun. Soil Sci. Plant Anal. 6 (5), 489–494.

Anderson, J.L., Bouma, J., 1977a. Water movement through pedal soils: I. Saturated flow. Soil Sci. Soc. Am. J. 41, 413–418.

Anderson, J.L., Bouma, J., 1977b. Water movement through pedal soils: II. Unsaturated flow. Soil Sci. Soc. Am. J. 41, 419–423.

Angulo-jaramillo, R., Gaudet, J.P., Thony, J.L., Vauclin, M., 1996. Measurement of hydraulic properties and mobile water content of a field soil. Soil Sci. Soc. Am. J. 60, 710–715.

Anomosa, P.R., Nikedi-Kizza, P., Blue, W.G., Sartain, J.B., 1990. Water movement through an aggregated, gravelly soil from Cameron. Geoderma 46, 263–281.

Beven, K., Germann, P., 1982. Macropores and water flow in soils. Water Resour. Res. 18, 1311–1325.

Biggar, J.W., Nielsen, D.R., 1962. Miscible displacement: II. Behavior of tracers. Soil Sci. Soc. Proc. 25, 1–25.

Blake, G.R., Hartge, K.H., 1986. Bulk density. In: Klute, A. (Ed.), Methods of Soil Analyses, Part 1. Physical and Mineralogical Methods, 2nd edn. Monogr. 9. ASA and SSSA, Madison, WI, pp. 363–375.

Booltink, H.W., Bouma, G.J., Gimenez, D., 1991. Suction crust infiltrometer for measuring hydraulic conductivity of unsaturated soil near saturation. Soil Sci. Soc. Am. J. 55, 566–568.

Bouma, J., 1977. Soil Survey and Study of Water in Unsaturated Soil. Soil Survey Papers, vol. 13. Netherlands Soil Survey Institute, Wageningen.

Bouma, J., 1991. Influence of soil macroporosity on environmental quality. Adv. Agron. 46, 1–32.

Brusseau, M.L., 1993. The influence of solute size, pore water velocity, and intraparticle porosity on solute dispersion and transport in soil. Water Resour. Res. 29, 1071–1080.

Brusseau, M.L., Rao, P.S.C., 1990. Modeling solute transport in structured soils: a review. Geoderma 46, 169–192.

Busacca, A.J., Montgomery, J.A., 1992. Field-landscape variation in soil physical properties of the Northwest Dryland Crop Production Region. In: Veseth, R., Miller, B. (Eds.), Precision Farming for Profit and Conservation, Proc. 10th Inland Northwest Conservation Farming Conference. Washington State University, Pullman, pp. 8–18.

Casey, F.X.M., Logsdon, S.D., Horton, R., Jaynes, D.B., 1998. Measurement of field soil hydraulic and solute transport parameters. Soil Sci. Soc. Am. J. 62, 1172–1178.

Donaldson, N.C., 1980. Soil survey of Whitman County, Washington. USDA, SCS and Washington State Univ. Agric. Res. Center, US Government Printing Office, Washington, DC.

Ersahin, S., 1996. Solute transport in sloping layered soils. PhD dissertation, Washington State University, Pullman, WA, USA.

Gee, G.W., Bouder, J.W., 1986. Particle-size analysis. In: Klute, A. (Ed.), Methods of Soil Analyses, Part 1. Physical and Mineralogical Methods, 2nd edn. Monogr. 9. ASA and SSSA, Madison, WI, pp. 383–409.

Gillman, G.P., 1979. A proposed method for the measurement of exchange properties of highly weathered soils. Aust. J. Soil Res. 16, 67–77.

Jackson, M.L., 1956. Soil Analysis Department of Soil Science, University of Wisconsin, Madison, WI Adv. Course, Fourth Printing.

Jardine, P.M., Jacobs, G.K., Wilson, G.V., 1993. Unsaturated transport processes in undisturbed heterogeneous porous media: I. Inorganic contaminants. Soil Sci. Soc. Am. J. 57, 945–953.

Klute, A., 1986. Water retention: laboratory methods. In: Klute, A. (Ed.), Methods of Soil Analyses. Part 1. Physical and Mineralogical Methods, 2nd edn. Monogr. 9. ASA and SSSA, Madison, WI, pp. 635–660.

Langner, H.W., Gaber, H.M., Wraith, J.M., Huwe, B., Inskeep, W.P., 1999. Preferential flow through intact soil cores: effects of matric head. Soil Sci. Soc. Am. J. 63, 1591–1598.

Li, Y., Ghodrati, M., 1994. Preferential flow of nitrate through soil columns containing root channels. Soil Sci. Soc. Am. J. 58, 653–659.

Luxmoore, R.J., 1981. Micro-, meso-, and macroporosity of soils. Soil Sci. Soc. Am. J. 45, 671–672.

McLean, E.O., 1982. Soil pH and lime requirement. In: Page, A.L. (Ed.), Methods of Soil Analysis, Part 2, 2nd edn. Monogr. 9. ASA and SSSA, Madison, WI, pp. 199–224.

Nielsen, D.R., Biggar, J.W., 1962. Miscible displacement: III. Theoretical considerations. Soil Sci. Soc. Am. Proc. 26, 216–221.

Nikedi-Kizza, P., Biggar, J.W., van Genuchten, M.Th., Wierenga, P.J., Selim, H.M., Davidson, J.M., Nielsen, D.R., 1983. Modeling tritium and chloride 36 transport through an aggregated oxisol. Water Resour. Res. 19, 691–700.

Parker, J.C., van Genuchten, M.Th., 1984. Determining transport parameters from laboratory and field tracer experiments. Bulletin 84-3 Virginia Agric. Exp. St., Blacksburg.

Rao, P.S.C., Jessup, R.E., Rolston, D.E., Davidson, J.M., Kilcrease, D.P., 1980. Experimental and mathematical

description of nonsorbed solute transport by diffusion in spherical aggregates. Soil Sci. Soc. Am. J. 44, 684–688.

Rasmuson, A., 1985. The influence of particles of variable size, shape, and properties on the dynamics of fixed beds. Chem. Eng. Sci. 40, 621.

Ranken, D.W., 1974. Hydrologic properties of soil and subsoil on a steep forested slope. Masters thesis, Oregon State University, Corvallis.

Rhoades, J.D., 1982. Soluble salts. In: Page, A.L. (Ed.), Methods of Soil Analysis. Part 2, 2nd edn. Monogr. 9. ASA and SSSA, Madison, WI, pp. 167–197.

Seyfried, M.S., Rao, P.S.C., 1987. Solute transport in undisturbed columns of an aggregated tropical soil: preferential effects. Soil Sci. Soc. Am. J. 51, 1334–1344.

Sugita, F., Gillham, R.W., 1995. Pore scale variations in retardation factor as a cause of nonideal reactive breakthrough curves: 1. Conceptual model and its evaluation. Water Resour. Res. 31, 103–112.

Toride, N., Leij, F.J., van Genuchten, M.Th., 1995. The CXTFIT code for estimating transport parameters from laboratory or field tracer experiments. Res. Rep. no. 137, US Salinity Lab., USDA, ARS, Riverside, CA.

van Genuchten, M.Th., 1981. Non-equilibrium transport parameters from miscible displacement experiments. Res. Rep. no. 119, US Salinity Lab., USDA, ARS, Riverside, CA.

van Genuchten, M.Th., Wierenga, P.J., 1977. Mass transfer in sorbing porous media: II. Experimental evaluation with tritium ($^3H_20$). Soil Sci. Soc. Am. J. 41, 272–278.

Wierenga, P.J., Black, R.J., Manz, P., 1973. A multichannel syringe pump for steady-state flow in soil columns. Soil Sci. Soc. Am. Proc. 37, 133–135.